

BBA 47618

## THE ORIENTATIONS OF TRANSITION MOMENTS IN REACTION CENTERS OF *RHODOPSEUDOMONAS SPHAEROIDES*, COMPUTED FROM DATA OF LINEAR DICHROISM AND PHOTOSELECTION MEASUREMENTS

RODERICK K. CLAYTON <sup>a</sup>, CHARLES N. RAFFERTY <sup>a</sup> and ANDRÉ VERMEGLIO <sup>b</sup>

<sup>a</sup> *Section of Botany, Genetics and Development, Cornell University, Ithaca, NY 14853 (U.S.A.)* and <sup>b</sup> *Département de Biologie, Service de Biophysique, Centre d'Etudes Nucléaires de Saclay, BP 2, 91190 Gif-sur-Yvette (France)*

(Received June 8th, 1978)

*Key words:* Bacteriochlorophyll; Bacteriopheophytin; Linear dichroism; Transition moment; Reaction center; (*Rhodopseudomonas sphaeroides*)

### Summary

Linear dichroism measurements of reaction centers of *Rhodopseudomonas sphaeroides* in stretched gelatin films have yielded angles that various optical transition moments make with an axis of symmetry in the reaction center. Photoselection experiments have yielded angles that certain transition moments make with each other. We have combined these data so as to compute the orientations of the  $Q_x$  and  $Q_y$  transition moments of the two molecules of bacteriopheophytin and of the bacteriochlorophyll special pair (photochemical electron donor) in the reaction center. Orientations are expressed in spherical polar coordinates with the symmetry axis as the pole. We have also computed additional angles between pairs of transition moments. In this treatment we have assumed that the bacteriopheophytins are independent monomers with little or no exciton coupling.

### Introduction

The photochemical reaction center of *Rhodopseudomonas sphaeroides* is a chromoprotein in which four molecules of bacteriochlorophyll and two of bacteriopheophytin are bound non-covalently to a protein composed of three polypeptides, weighing about  $8 \cdot 10^4$  daltons [1]. Partial information about the orientations of the chromophores, in relation to each other and to the photosynthetic membrane, has been obtained by the photoselection technique [2] and by measuring optical linear dichroism in oriented preparations [3–5]. In dried gelatin films [5], reaction centers are oriented randomly with respect to rotation about an axis \* in the reaction center; this axis of symmetry lies pre-

---

\* This axis is not necessarily a property of a single reaction center. It could, for example, arise from the interactions of specific surface binding sites, forming linear aggregates of reaction centers. But in that case the binding sites define a particular axis in each reaction center, related to the axis of the aggregate.

ferentially in the plane of the film. When such films are humidified, stretched and dried again, the axes of symmetry tend to become aligned with the direction of stretching. In strongly stretched films this alignment approaches a limit of perfect orientation, with axial symmetry about the stretching direction. In this limit, the angle  $\theta$  between a transition dipole and the axis of symmetry is given by  $A_{\parallel}/A_{\perp} = 2 \cos^2 \theta$ , where  $A_{\parallel}$  and  $A_{\perp}$  are the absorbances measured with the electric vector of the measuring light parallel and perpendicular to the direction of stretching, respectively. We [6] determined values of  $\theta$  for transition moments of the two molecules of bacteriopheophytin and for the bacteriochlorophyll ('special pair') that acts as photochemical electron donor. In a separate study [2], the photoselection technique was applied to determine the angles that some of these transition moments make with each other. These data are supplemented by new photoselection measurements\*. We show here that by combining these data we can specify the orientations of transition moments in a spherical polar coordinate system with the axis of symmetry as the pole.

### Mathematical treatment

Imagine a spherical coordinate system in which the axis of symmetry of the reaction center, as defined by the experiments with stretched gelatin films, is the pole. The orientation of a transition dipole can be represented by a vector drawn from the center and terminating on the surface of a unit sphere. The terminus has coordinates  $\theta$  (declination from pole) and  $\phi$  (longitude). We arbitrarily set  $\phi = 0$  for the 870 nm transition moment of special pair bacteriochlorophyll (for this transition,  $\theta = 41 \pm 1^\circ$  [5]).

Fig. 1 shows the 870 nm transition moment and two other transition moments from a polar perspective. Great circle lines are drawn on the surface of the sphere connecting the terminus of each transition moment and the north pole. The angle between the two transition moments is  $\gamma_{12}$ . Then the law of cosines in spherical trigonometry gives

$$\cos \gamma_{12} = \cos \theta_1 \cos \theta_2 + \sin \theta_1 \sin \theta_2 \cos(\phi_2 - \phi_1)$$

Note that there is redundancy in that a transition moment with coordinates  $\theta$ ,  $\phi$  also has coordinates  $(180^\circ - \theta)$ ,  $(180^\circ + \phi)$  as it intersects the opposite side of the sphere. Also the angle  $180^\circ - \gamma_{12}$  is redundant to  $\gamma_{12}$  as an expression of the angle between two transition moments.

We shall proceed from the known values of  $\theta$  [5] and  $\gamma$  [2] to compute values of  $\phi$ , and then in some cases to compute other values of  $\theta$  and  $\gamma$ . The two sets of data [2,5] will be seen to be quantitatively compatible. In some instances the requirement of at least approximate compatibility removes ambiguities of plus and minus sign that arise when the law of cosines is applied.

---

\* Methodological details in these new photoselection measurements are essentially as described by Vermeglio et al. [2]; they will be described in a later publication.

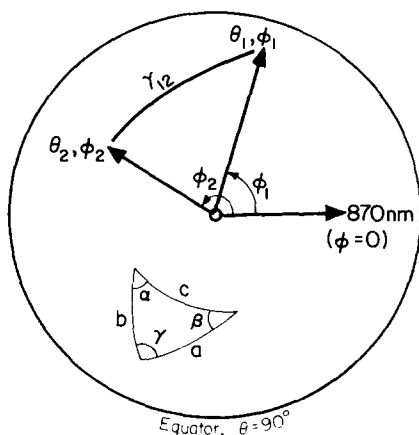


Fig. 1. Polar view of a spherical coordinate system with the axis of symmetry of a reaction center (see the text) as the pole. Optical transition moments are represented by vectors drawn from the center to the surface of the sphere. The 870 nm transition moment is set arbitrarily at  $\phi = 0$ . Two other transition moments are shown. Great circles on the sphere connect the terminus of each transition moment and the pole. The angle between the transition moments is  $\gamma_{12}$ . For any great circle triangle,  $\cos a = \cos b \cos c + \sin b \sin c \cos \alpha$ , where the Roman letters denote angles subtended at the center and the greek letters denote interior angles of the triangle on the surface of the sphere.

## Computations

### Transition moments

The two molecules of bacteriopheophytin in a reaction center have absorption bands at 530 and 545 nm ( $Q_x$  transitions), resolved at low temperature [7], and a band near 760 nm (unresolved  $Q_y$  transitions). We treat these molecules as independent monomers with little or no exciton coupling, for three principal reasons: (1) Small light-induced shifts of the 760 nm band, concomitant to photochemical activity, are different in shape in photoselection experiments, depending on whether they are excited by 530 or 545 nm light [2]. This would not be expected if the  $Q_x$  transitions at 530 and 545 nm arise from dimeric exciton splitting. (2) A transient intermediate state in the photochemistry is characterized by bleaching of the 545 nm band [8], ascribed to reduction of the '545 nm' bacteriopheophytin molecule, and unrelated to the aforementioned band shifts. When the 545 nm band is bleached, the 530 nm band remains unperturbed. (3) Circular dichroism spectra [9,10] do not show bands of opposite sign in either the 530–545 nm region or the 760 nm region. We therefore assume that each bacteriopheophytin behaves like a monomer, with  $Q_x$  and  $Q_y$  transitions at 545 and 760 nm for one and at 530 and 760 nm for the other. In each monomer the  $Q_x$  transition moment is perpendicular to the  $Q_y$  transition moment, and both are in the tetrapyrrole plane of the molecule. For convenience we shall denote these transitions as  $PX_1$  (545 nm) and  $PY_1$  (760 nm) for the one bacteriopheophytin, and  $PX_2$  (530 nm) and  $PY_2$  (760 nm) for the other.

The photo-oxidation of the bacteriochlorophyll 'special pair' results in the disappearance of absorption bands centered at 600, 630, 805 and about

870 nm. (The band near 870 nm varies between 850 and 870 nm depending on the environment of the reaction center; we shall refer to it generically as the 870 band) [2,3,5]. A simple interpretation of these bands is that they arise from dimeric exciton (transition dipole) coupling of the two molecules of bacteriochlorophyll that comprise the special pair. The bands at 600 and 630 nm then represent the  $Q_x$  transitions of the dimer, and those at 805 and 870 nm the  $Q_y$  transitions. Molecular exciton theory [11,12] predicts that the two  $Q_x$  transition moments are mutually perpendicular, and so are the two  $Q_y$  transition moments. Other interpretations are of course possible; for example the bands could arise through exciton interactions between the special pair and the other tetrapyrroles in the reaction center. We shall denote the transition moments at 870, 805, 625 and 600 nm as  $BY_1$ ,  $BY_2$ ,  $BX_1$  and  $BX_2$  respectively.

Data

Values of  $\theta$  for various transition moments, determined earlier [5], are shown in Table I. Angles between various pairs of transition moments, determined by photoselection (ref. 2 and this report), are shown in Table II. In the bacteriopheophytin monomers,  $PX_1 \perp PY_1$  and  $PX_2 \perp PY_2$ . Note that the angle of  $90^\circ$  between  $BX_1$  and  $BX_2$  is consistent with molecular exciton theory applied to the bacteriochlorophyll special pair as a dimer.

The two bacteriopheophytins

The  $Q_x$  transition moments of the two bacteriopheophytin molecules of the reaction center,  $PX_1$  (545 nm) and  $PX_2$  (530 nm), together with  $BY_1$  (870 nm), are sketched in Fig. 2a. This sketch is like the one in Fig. 1 except that the drawing has been stylized by representing all of the great circle segments as straight lines. Numerical values of the angles (excluding the confidence limits), shown on the sketch, are from Tables I and II. The axis of symmetry is labeled A. For the two triangles in this sketch the law of cosines gives

$$\cos(60 \text{ or } 120) = \cos 46 \cos 41 + \sin 46 \sin 41 \cos \phi_1$$

TABLE I  
THE ANGLE  $\theta$  BETWEEN VARIOUS TRANSITION MOMENTS AND AN AXIS OF SYMMETRY IN REACTION CENTERS OF *R. SPHAEROIDES*

Data taken from Rafferty and Clayton [5]. In this reference the angle was called  $\alpha$ .

Wavelength (nm)	Chromophore	Transition	Designation	$\theta$ (degrees)
530	One bacteriopheophytin	$Q_x$	$PX_2$	$46 \pm 1$
545	Other bacteriopheophytin	$Q_x$	$PX_1$	$46 \pm 1$
760	Both bacteriopheophytins	$Q_y$	$PY_1, PY_2$ (unresolved)	$61 \pm 1$ (average)
600	Bacteriochlorophyll special pair	$Q_x$	$BX_2$	$64 \pm 1$
630	Bacteriochlorophyll special pair	$Q_x$	$BX_1$	$22.5 \pm 3$
805	Bacteriochlorophyll special pair	$Q_y$	$BY_2$	—
855 (generically "870")	Bacteriochlorophyll special pair	$Q_y$	$BY_1$	$41 \pm 1$

TABLE II

ANGLES BETWEEN VARIOUS PAIRS OF TRANSITION MOMENTS IN REACTION CENTERS OF *R*. SPHAEROIDES

Data taken from Vermeglio et al. [2] and from new data in this report (C.N.R.). Conservative estimates of confidence limits have been added. The designations of transitions are explained in Table I.

Wavelengths (nm)	Transition no. 1	Transition no. 2	Angle $\gamma_{12}$ (degrees) between the transition moments
530, 760	$PX_2$	$PY_2$	90; orthogonal in monomer
545, 760	$PX_1$	$PY_1$	90; orthogonal in monomer
530, 760	$PX_2$	$PY_1$	$51 \pm 2$ or $129 \pm 2$
545, 760	$PX_1$	$PY_2$	$46 \pm 2$ or $134 \pm 2$
760	$PY_1$	$PY_2$	$55 \pm 2$ or $125 \pm 2$
530, 870	$PX_2$	$BY_1$	$50 \pm 2$ or $130 \pm 2$
545, 870	$PX_1$	$BY_1$	$60 \pm 2$ or $120 \pm 2$
760, 870	$PY_1$ and $PY_2$ (unresolved)	$BY_1$	$90 \pm 20$
600, 870	$BX_2$	$BY_1$	68 or 112 [2], $75.5 \pm 3$ or $104.5 \pm 3$ (C.N.R.)
630, 870	$BX_1$	$BY_1$	$30.5 \pm 3$ or $149.5 \pm 3$ (C.N.R.)
600, 630	$BX_2$	$BX_1$	$90 \pm 15$ (C.N.R.)

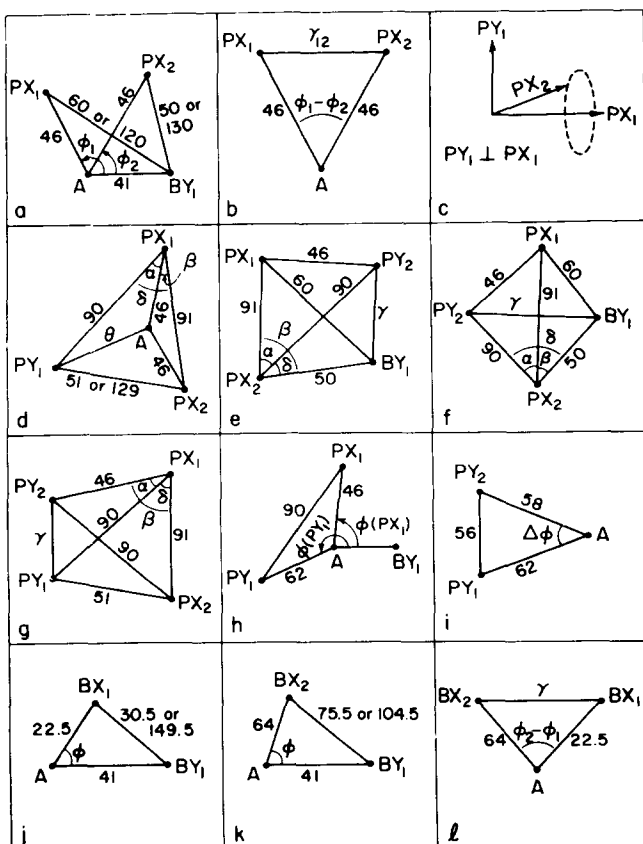


Fig. 2. Stylized drawings on which the various computations are based. Details are in the text. Angles are in degrees.

and

$$\cos(50 \text{ or } 130) = \cos 46 \cos 41 + \sin 46 \sin 41 \cos \phi_2$$

where all the angles are in degrees. Choosing 120 or 130° on the left side of these equations leads to  $|\cos \phi_1| > 1$  and  $|\cos \phi_2| > 1$ , so these values can be eliminated from further consideration. They would arise if we were to extend some transition moments into the southern hemisphere, replacing  $\theta$  by  $180^\circ - \theta$ , but such a treatment would be redundant to the present one. Solving the first of these equations, including the confidence limits listed in Tables I and II, gives  $\phi_1 = \phi(PX_1) = 93 \pm 6^\circ$ . We have chosen the positive sign arbitrarily. The alternative,  $-93 \pm 6^\circ$ , would lead to a configuration that is the mirror image of the one we shall construct here. This alternative is mentioned in Discussion. The second equation gives  $\phi_2 = \phi(PX_2) = 75 \pm 5^\circ$ . Then in the sketch of Fig. 2b,  $\cos \gamma_{12} = \cos 46 \cos 46 + \sin 46 \sin 46 \cos(\phi_1 - \phi_2)$ . The choice of plus or minus sign for  $\phi(PX_2)$  gives  $\phi_1 - \phi_2 = 18 \pm 11^\circ$  and  $168 \pm 11^\circ$ , respectively; these in turn give  $\gamma_{12} = 14 \pm 7^\circ$  and  $91 \pm 1^\circ$ , respectively. The sketch of Fig. 2c shows how one of these alternatives can be eliminated. The orthogonal monomeric transition moments  $PX_1$  and  $PX_2$  are drawn as axes in a rectangular coordinate system; possible loci of  $PX_2$  describe a cone about  $PX_1$  with half-angle  $\gamma_{12}$ . The least possible angle between  $PY_1$  and  $PX_2$  is  $90^\circ - \gamma_{12}$ . If  $\gamma_{12} = 14 \pm 7^\circ$ , the angle between  $PX_2$  and  $PY_1$  can be no smaller than  $90 - 21$  or  $69^\circ$ , which contradicts the value of  $51^\circ$  in Table II. Similarly the least possible angle between  $PX_1$  and  $PY_2$  is  $69^\circ$ , contradicting the value of  $46^\circ$  in Table II. We therefore choose  $\phi(PX_2) = -75 \pm 5^\circ$ ; i.e.,  $285 \pm 5^\circ$ , and  $\gamma(PX_1, PX_2) = 91 \pm 1^\circ$ . This value of  $\gamma_{12}$  places no constraints on the angle between  $PX_2$  and  $PY_1$ , or between  $PX_1$  and  $PY_2$ .

We shall now compute the  $\theta$  coordinates of  $PY_1$  and  $PY_2$ ; these can be compared with our average value of  $61 \pm 1^\circ$  (Table I). We use the sketch of Fig. 2d, which includes numerical values from Tables I and II and  $\gamma(PX_1, PX_2) = 91^\circ$ . Applying the law of cosines to triangle  $PY_1, PX_1, PX_2$ , the angle  $\delta$  is  $51 \pm 2^\circ$  or  $129 \pm 2^\circ$  depending on whether  $\gamma(PY_1, PX_2)$  is taken as  $51^\circ$  or  $129^\circ$ . The angle  $\beta$ , from triangle  $A, PX_1, PX_2$ , is  $11 \pm 11^\circ$ . Then  $\alpha = \delta - \beta = 40 \pm 13^\circ$  or  $118 \pm 13^\circ$ . From triangle  $PY_1, PX_1, A$  the law of cosines gives  $\theta(PY_1) = 58 \pm 7^\circ$  or  $110 \pm 7^\circ$ . We reject the latter value because it represents a redundant extension into the southern hemisphere. Therefore we reject  $\gamma(PY_1, PX_2) = 129^\circ$ , keeping only the value  $51^\circ$ . Following the same treatment with  $PY_2$  in place of  $PY_1$  and angles  $\alpha$ ,  $\beta$ , and  $\delta$  measured around  $PX_2$  instead of  $PX_1$ , we find  $\theta(PY_2) = 55 \pm 6^\circ$  and we reject  $\gamma(PY_2, PX_1) = 134^\circ$ , keeping only the value  $46^\circ$ . These values of  $\theta$  are compatible with the average  $\theta(PY_1$  and  $PY_2)$  of  $61 \pm 1^\circ$ , listed in Table I. If we restrict  $\theta(PY_1)$  and  $\theta(PY_2)$  to values for which their average can be  $61 \pm 1^\circ$ , we obtain  $\theta(PY_1) = 62 \pm 3^\circ$  and  $\theta(PY_2) = 58 \pm 3^\circ$ .

In Fig. 2d we could have drawn  $PY_2$  pointing to the right from A. The angles  $\alpha$ ,  $\beta$  and  $\delta$  would then have been related by  $\alpha = \delta + \beta$ , giving larger values of  $\theta$ . We will show later that both  $PY_1$  and  $PY_2$  must fall to the left of the ' $PX_1, A, PX_2$ ' plane in this polar view, so this alternative representation can be ignored.

We shall now compute the angles that  $PY_1$  and  $PY_2$  make with  $BY_1$ , without using the value  $90 \pm 20^\circ$  listed for these angles in Table II. Figs. 2e and 2f show

alternative sketches with data from Table II and  $\gamma(PX_1, PX_2) = 91^\circ$  as computed earlier. For Fig. 2e the law of cosines gives  $\alpha = 46 \pm 2^\circ$ ,  $\beta = 50 \pm 4^\circ$ , and consequently  $\delta = 4 \pm 6^\circ$ . (The symbols  $\alpha$ ,  $\beta$  and  $\delta$  do not necessarily refer to the same angles in the various sketches of Fig. 2; the same symbols are used in different contexts for convenience.) Then from triangle  $PX_2, PY_2, BY_1$  we compute  $\gamma(PY_2, BY_1) = 40 \pm 2^\circ$ , incompatible with the value  $90 \pm 20^\circ$  in Table II. For Fig. 2f we obtain  $\delta = 96 \pm 6^\circ$  and  $\gamma(PY_2, BY_1) = 95 \pm 5^\circ$ , compatible with  $\gamma = 90 \pm 20^\circ$ . Using similar diagrams with  $PY_1$  in place of  $PY_2$  and angles  $\alpha$ ,  $\beta$  and  $\delta$  measured about  $PX_1$  instead of  $PX_2$ , we find  $\gamma(PY_1, BY_1) = 35 \pm 4^\circ$  (incompatible) for the arrangement of Fig. 2e and  $85 \pm 5^\circ$  (compatible) for the arrangement of Fig. 2f. We therefore place  $PY_1$  and  $PY_2$  in the same hemisphere relative to the plane containing  $PX_1$  and  $PX_2$ , and we put  $BY_1$  in the opposite hemisphere; that is, we choose the configuration of Fig. 2f and confirm the configuration of Fig. 2d.

Next we will compute the angle between  $PY_1$  and  $PY_2$  and compare the result with the value  $55^\circ$  or  $125^\circ$  listed in Table II. We use a three-step calculation using the triangles sketched in Fig. 2g. Alternative sketches with  $PY_1$  and/or  $PY_2$  to the right of the ' $PX_1, PX_2$ ' plane have been ruled out. We will show later that  $\phi(PY_1) > \phi(PY_2)$ , which rules out the interchange of  $PY_1$  and  $PY_2$  in Fig. 2g. The known angles on this sketch include values from Table II and  $\gamma(PY_1, PX_2) = 91^\circ$ . The law of cosines applied to the triangles  $PX_2, PX_1, PY_2$  and  $PX_2, PX_1, PY_1$  gives  $\beta = 89 \pm 1^\circ$  and  $\delta = 51 \pm 2^\circ$ . The angle  $\alpha$  is then  $38 \pm 3^\circ$ . Having determined  $\alpha$  in Fig. 2g, we can apply the law of cosines to triangle  $PY_1, PX_1, PY_2$ , giving  $\gamma(PY_1, PY_2) = 56 \pm 2^\circ$ , in agreement with the value  $55^\circ$  (Table II) that was not used in this computation \*.

Now for the  $\phi$  coordinates of  $PY_1$  and  $PY_2$ , refer to Fig. 2h. Triangle  $PY_1, A, PX_1$  gives  $\phi(PY_1) - \phi(PX_1) = 121 \pm 5^\circ$ . Then with  $\phi(PX_1) = 93 \pm 6^\circ$  as computed earlier,  $\phi(PY_1) = 214 \pm 11^\circ$ . A similar computation using triangle  $PY_2, A, PX_2$  gives  $\phi(PY_2) = 157 \pm 12^\circ$ . The two values of  $\phi$  differ by  $57 \pm 23^\circ$ . As a cross-check we can compute this difference,  $\phi(PY_1) - \phi(PY_2)$ , from the triangle  $PY_1, A, PY_2$  (Fig. 2i); the result is  $65 \pm 5^\circ$ . With this restriction we can narrow the limits of  $\phi(PY_1)$  and  $\phi(PY_2)$  slightly;  $\phi(PY_1) = 215 \pm 10^\circ$  and  $\phi(PY_2) = 155 \pm 10^\circ$ .

### *The bacteriochlorophyll special pair*

Angles involving the bacteriochlorophyll special pair transition moments  $BX_1$  (630 nm),  $BX_2$  (600 nm) and  $BY_1$  (870 nm) are shown in Figs. 2j and 2k. The angle between  $BX_2$  and  $BY_1$  is shown as  $75.5^\circ$  or  $104.5^\circ$ ; Table II lists these values along with the alternative  $68^\circ$  or  $112^\circ$  [2]. We prefer the former pair of values because they have been corrected for trivial sources of depolarization in their measurement.

The  $\phi$  coordinates of  $BX_1$  and  $BX_2$  can be found by applying the law of cosines to the triangles in Figs. 2j and 2k. If  $\gamma(BY_1, BY_1)$  is given the value

\* If we had chosen  $\gamma(PX_1, PX_2) = 14 \pm 1^\circ$  instead of  $91 \pm 1^\circ$ , ignoring the fact that this choice is incompatible with  $\gamma(PX_2, PY_1) = 51^\circ$  and  $\gamma(PX_1, PY_2) = 46^\circ$  (see earlier), we could have made an independent estimate of  $\gamma(PY_1, PY_2)$ , using other angles involving  $PX_1$ ,  $PX_2$ ,  $PY_1$ ,  $PY_2$  and the axis of symmetry in a three step application of the law of cosines. Such a calculation (not shown here) gives  $\gamma(PY_1, PY_2) < 27^\circ$ , which conflicts with the value of  $55^\circ$  listed in Table II.

149.5° (Fig. 2j) we are led to the impossible condition  $|\cos \phi| > 1$ , so we reject this value and keep only  $\gamma(BX_1, BY_1) = 30.5^\circ$ . We then find  $\phi(BX_1) = \pm 50 \pm 10^\circ$ ; we have no basis for preferring the positive or the negative sign. Turning to Fig. 2k we cannot exclude either value of  $\gamma(BX_2, BY_1)$ . The value of 75.5° leads to  $\phi(BX_2) = \pm 98 \pm 7^\circ$ , while the value of 104.5° gives  $\phi(BX_2) = \pm 163 \pm 17^\circ$ .

The multiplicity of alternative positive and negative signs in these  $\phi$  coordinates can be reduced through calculations based on Fig. 2l. We require that  $\gamma(BX_1, BX_2)$ , as computed from  $\phi_2 - \phi_1$  through the law of cosines, must fall within the range  $90 \pm 15^\circ$  determined experimentally. In these computations  $\phi_1 = \phi(BX_1) = \pm 50 \pm 10^\circ$ . For  $\gamma(BX_2, BY_1) = 75.5^\circ$ , we have  $\phi_2 = \phi(BX_2) = \pm 98 \pm 7^\circ$ . Then if  $\phi_1$  and  $\phi_2$  have the same sign,  $\phi_2 - \phi_1 = \pm 48 \pm 17^\circ$ , and we compute  $\gamma(BX_1, BX_2) = 51 \pm 7^\circ$ , in contradiction to the measured value. If  $\phi_1$  and  $\phi_2$  have opposite signs,  $\phi_2 - \phi_1 = \pm 148 \pm 17^\circ$  and  $\gamma(BX_1, BX_2) = 83 \pm 7^\circ$ , in agreement with the measured value of  $90 \pm 15^\circ$ . Now for the case that  $\gamma(BX_2, BY_1) = 104.5^\circ$  and  $\phi_2 = \pm 163 \pm 17^\circ$ , we have  $\phi_2 - \phi_1 = \pm 113 \pm 27^\circ$  when  $\phi_1$  and  $\phi_2$  have the same sign, and  $\pm 213 \pm 17^\circ$  with opposite sign. From these values we compute  $\gamma(BX_1, BX_2) = 73 \pm 10^\circ$  (same sign) or  $83 \pm 8^\circ$  (opposite signs), the former in marginal agreement and the latter in complete agreement with the measured value. We therefore choose opposite signs for  $\phi(BX_1)$  and  $\phi(BX_2)$  in every case. In summary, we list the following possibilities: If

$$\gamma(BX_2, BY_1) = 75.5^\circ,$$

$$\phi(BX_2) = \pm 98 \pm 7^\circ \text{ and } \phi(BX_1) = \mp 50 \pm 10^\circ.$$

If

$$\gamma(BX_2, BY_1) = 104.5^\circ,$$

$$\phi(BX_2) = \pm 163 \pm 17^\circ \text{ and } \phi(BX_1) = \mp 50 \pm 10^\circ$$

Finally we can compute the angles that  $BX_1$  and  $BX_2$  make with all four transition moments of bacteriopheophytin, applying the law of cosines to the

TABLE III

POLAR COORDINATES (SEE FIG. 1) OF TRANSITION MOMENTS IN REACTION CENTERS OF *R. SPHAEROIDES*

Computed from the data of Tables I and II. Angles are in degrees. Designations of transitions are explained in Table I.  $BY_1$  was set at  $\phi = 0$ . Wavelengths of transitions in nm are shown in parentheses.

Transition	$\theta$	$\phi$
$BY_1$ (870)	$41 \pm 1^*$	0
$BX_1$ (630)	$22.5 \pm 3^*$	$\pm 50 \pm 10$
$BX_2$ (600)	$64 \pm 1^*$	$\pm 98 \pm 7$ or $\pm 163 \pm 17^{**}$
$PY_1$ (760)	$62 \pm 3$	$215 \pm 10$
$PY_2$ (760)	$58 \pm 3$	$155 \pm 10$
$PX_1$ (545)	$46 \pm 1^*$	$93 \pm 6$
$PX_2$ (530)	$46 \pm 1^*$	$285 \pm 5$

\* Experimental values carried over from Table I.

\*\* The two sets of values of  $\phi(BX_2)$  result from two choices of the angle between  $BX_2$  and  $BY_1$ , 75.5° or 104.5°, respectively (see Table IV and the text). The sign of  $\phi(BX_2)$  must be taken opposite to that of  $\phi(BX_1)$ .



TABLE IV  
ANGLES BETWEEN PAIRS OF TRANSITION MOMENTS

Wavelengths of transitions in nm are shown in parentheses. Angles are in degrees. These are the angles between transition moments drawn in the northern hemisphere ( $\theta = 0$  to  $90^\circ$ ) of the coordinate system of Figs. 1 and 3. We omit redundant supplements of these angles involving projection of transition moments into the southern hemisphere. In one case ( $BY_1, BX_2$ ) both the angle and its supplement are allowed when transition moments are drawn only in the northern hemisphere.

First Transition	Second transition	Angle between the transition moments
$PX_1$ (545)	$BY_1$ (870)	$60 \pm 2^*$
	$PY_1$ (760)	$90^{**}$
	$PY_2$ (760)	$46 \pm 2^*$
	$PX_2$ (530)	$91 \pm 1$
$PX_2$ (530)	$BY_1$ (870)	$50 \pm 2^*$
	$PY_1$ (760)	$51 \pm 2^*$
	$PY_2$ (760)	$90^{**}$
$BY_1$ (870)	$PY_1$ (760)	$85 \pm 5$
	$PY_2$ (760)	$95 \pm 5$
	$BX_1$ (630)	$30.5 \pm 3^*$
	$BX_2$ (600)	$75.5 \pm 3$ or $104.5 \pm 3^*$
$PY_1$ (760)	$PY_2$ (760)	$56 \pm 2$
$BX_1$ (630)	$BX_2$ (600)	$90 \pm 15^*$

\* Experimental values carried over from Table II.  
\*\* Theoretical (orthogonal transition moments in monomer).

TABLE V  
ADDITIONAL ANGLES BETWEEN PAIRS OF TRANSITION MOMENTS

The angles made with  $BX_1$  have two values corresponding to  $\phi(BX_1) = 50^\circ$  or  $-50^\circ$ . The angles made with  $BX_2$  have four values corresponding to  $\phi(BX_2) = \text{approx. } \pm 98^\circ$  or  $\text{approx. } \pm 163^\circ$  (see Table III and the text). These alternatives are restricted in that a positive sign for  $\phi(BX_1)$  must be coupled with a negative sign for  $\phi(BX_2)$  and vice versa. Angles are in degrees.

First transition	Second transition	Angle between transition moments	
		$\phi(BX_1) = 50^\circ$	$\phi(BX_1) = -50^\circ$
$BX_1$ (630)	$PY_1$ (760)	$83 \pm 8$	$67 \pm 11$
	$PY_2$ (760)	$66 \pm 11$	$78 \pm 8$
	$PX_1$ (545)	$34 \pm 5$	$64 \pm 6$
	$PX_2$ (530)	$61 \pm 7$	$29 \pm 3$
$BX_2$ (600)	$PY_1$ $PY_2$ $PX_1$ $PX_2$	$\phi(BX_2) = -98^\circ$	$\phi(BX_2) = 98^\circ$
		$42 \pm 16$	$98 \pm 14$
		$89 \pm 14$	$50 \pm 15$
		$108 \pm 4$	$21 \pm 2$
		$27 \pm 7$	$109 \pm 3$
$BX_2$	$PY_1$ $PY_2$ $PX_1$ $PX_2$	$\phi(BX_2) = -163^\circ$	$\phi(BX_2) = 163^\circ$
		$20 \pm 20$	$46 \pm 24$
		$37 \pm 23$	$18 \pm 13$
		$81 \pm 15$	$58 \pm 17$
		$71 \pm 16$	$91 \pm 13$

polar coordinates already determined for these transition moments. We use each of the alternative sets of values for  $\gamma(BX_2, BY_1)$ ,  $\phi(BX_1)$  and  $\phi(BX_2)$ . The results of these computations are listed in Table V. Other data are recapitulated in Tables III and IV.

## Discussion

The major results of this study are shown pictorially in Fig. 3. The solid and dashed vectors labeled '600' show the different orientations of  $BX_2$  that arise when  $\gamma(BX_2, BY_1)$  is taken as  $75.5$  or  $104.5^\circ$ . An alternative picture, equally acceptable, would have the sign of  $\phi$  reversed for both  $BX_2$  (600 nm) and  $BX_1$  (630 nm). And for each of these pictures we can visualize a mirror image, again equally acceptable, in which  $\phi$  has been changed to  $-\phi$  for all the transition moments.

For the transition moments in Fig. 3, the numerical values of their coordinates are listed in Table III. For completeness we repeat some of the content of Tables I and II. Angles between pairs of transition moments are shown in Tables IV and V.

The integrated absorption band intensity of  $BY_1$  (870 nm) is at least five times that of  $BY_2$  (805 nm), and that of  $BX_2$  (600 nm) is at least five times that of  $BX_1$  (630 nm) [2,5]. Thus, the transition of lower energy is favored in the  $Q_y$  region, and that of higher energy is favored in the  $Q_x$  region. Molecular exciton theory [11,12] applied to the bacteriochlorophyll special pair as a dimer then predicts that the component monomer  $Q_y$  transition moments are parallel within about  $40^\circ$  and predominantly collinear, while the monomer  $Q_x$

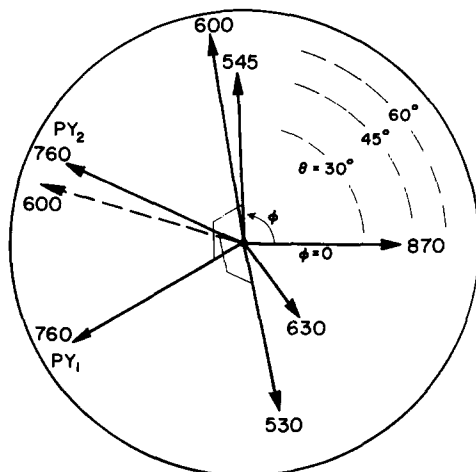


Fig. 3. Polar view of the orientations of optical transition moments in reaction centers of *R. sphaeroides*, in a spherical coordinate system with an axis of symmetry of the reaction center as the pole. The numerals at the ends of the transition moments denote wavelength in nm. These transition moments are identified in the text. Two alternative orientations of the 600 nm transition moment are indicated by the solid and dashed vectors labeled 600. Another configuration, equally acceptable, has the sign of  $\phi$  reversed for both the 600 and 630 nm transitions. Beyond that, an equally acceptable picture would be a mirror image with  $-\phi$  in place of  $\phi$  for all the transition moments. Numerical values of  $\theta$  and  $\phi$  are given in Table III.

transition moments are parallel within about  $40^\circ$  and predominantly side by side. We have no information about the translational coordinates of these chromophores, but these conclusions coupled with the coordinates we have obtained are not incompatible with current theoretical models [13] of the special pair. We acknowledge that the treatment of the special pair as an exciton-coupled dimer is nothing more than a simple working hypothesis; interactions with the other chromophores may also be responsible for the bands at 870, 805, 630 and 600 nm.

### Acknowledgements

This work was supported by Contract No. EY-76-S-02-3162 with the U.S. Department of Energy and by Grant No. 78-11102 from the National Science Foundation.

### References

- 1 Clayton, R.K. (1978) in *The Photosynthetic Bacteria* (Clayton, R.K. and Sistrom, W.R., eds.), Chapt. 20, Plenum Publishing Corp., New York, in press
- 2 Vermeglio, A., Breton, J., Paillotin, G. and Cogdell, R. (1978) *Biochim. Biophys. Acta* 501, 514—530
- 3 Vermeglio, A. and Clayton, R.K. (1976) *Biochim. Biophys. Acta* 449, 500—515
- 4 Rafferty, C.N. and Clayton, R.K. (1978) *Biochim. Biophys. Acta* 502, 51—60
- 5 Rafferty, C.N. and Clayton, R.K. (1979) *Biochim. Biophys. Acta* 545, 106—121
- 6 Norris, J.R., Uphaus, R.A., Crespi, H.L. and Katz, J.J. (1973) *Proc. Natl. Acad. Sci. U.S.* 68, 625—628
- 7 Clayton, R.K. and Yamamoto, T. (1976) *Photochem. Photobiol.* 24, 67—70
- 8 Rockley, M.G., Windsor, M.W., Cogdell, R.J. and Parson, W.W. (1975) *Proc. Natl. Acad. Sci. U.S.* 72, 2251—2255
- 9 Sauer, K., Dratz, E.A. and Coyne, L. (1968) *Proc. Natl. Acad. Sci. U.S.* 61, 17—24
- 10 Reed, D.W. and Ke, B. (1973) *J. Biol. Chem.* 248, 3041—3045
- 11 Kasha, M. (1963) *Radiat. Res.* 20, 55—71
- 12 Kasha, M., Rawls, H.R. and El-Bayoumi, M.A. (1965) *Pure Appl. Chem.* 11, 371—392
- 13 Katz, J.J., Norris, J.R. and Shipman, L.L. (1976) *Brookhaven Symp. Biol.* 28, 16—55